Dynamic scaling analysis of two-dimensional cell colony fronts in a gel medium: A biological system approaching a quenched Kardar-Parisi-Zhang universality

M. A. C. Huergo,[1,*] N. E. Muzzio,[1,†] M. A. Pasquale,[1,‡] P. H. Pedro González,[2,§] A. E. Bolzán,[1,‖] and A. J. Arvia[1,¶]

[1]*Instituto de Investigaciones Fisicoquímicas Teóricas y Aplicadas (INIFTA), (UNLP, CONICET),*

Sucursal 4, Casilla de Correo 16, 1900 La Plata, Argentina

[2]*Cátedra de Patología, Facultad de Ciencias Médicas, (UNLP, CIC), Calle 60 y 120, 1900 La Plata, Argentina*

The interfacial two-dimensional spreading dynamics of quasilinear Vero cell colony fronts in methylcellulose (MC)-containing culture medium, under a constant average front displacement velocity regime, was investigated. Under comparable experimental conditions, the average colony front displacement velocity becomes lower than that reported for a standard culture medium. Initially, the presence of MC in the medium hinders both the colony spreading, due to a gradual change in the average size and shape of cells and their distribution in the colony, and the cell motility in the gelled medium. Furthermore, at longer culture times enlarged cells appear at random in the border region of the colony. These cells behave as obstacles (pinning sites) for the displacement of smaller cells towards the colony front. The dynamic scaling analysis of rough fronts yields the set of exponents $\alpha = 0.63 \pm 0.04$, $\beta = 0.75 \pm 0.05$, and $z = 0.84 \pm 0.05$, which is close to that expected for a quenched Kardar-Parisi-Zhang model.

I. INTRODUCTION

The growth of cell colonies is a complex process that is usually studied with emphasis on either the physical or the biological characteristics of the system. In the former case, the statistical physics offers a possible framework for studying the propagation of cell colony fronts by means of the dynamic scaling theory [1]. This approach, in which the main measurement involved is the variance of the rough front height, has been extensively applied for investigation of the non-Euclidean behavior and the growth dynamics of one-dimensional (1D) to three-dimensional (3D) nonliving systems [2]. It has also been employed as an alternative insight for advancing the comprehension of the mechanism of bacterial [3,4] and cell line [5–10] colony spreading dynamics. The latter, unlike primary cells, continue growing and dividing as long as adequate culture conditions are maintained. Accordingly, the interfacial dynamics of each condensed system in a specific environment can be associated with a set of exponents (β, α, z, the growth, the roughness, and the dynamic exponent, respectively), which can be interpreted in terms of complex statistical models [1,2,7,11–13]. For Vero [8,9] and Hela [10] cell colonies growing in a standard culture medium, exhibiting either linear [8,10] or circular [9] two-dimensional (2D) growth fronts, the set of exponents $\alpha = 0.50 \pm 0.05$, $\beta = 0.32 \pm 0.04$, and $z = 1.56 \pm 0.10$, within certain colony age and size ranges, was obtained. This set is consistent with the Kardar-Parisi-Zhang (KPZ) universality class [1,2,14], despite the continuous spatiotemporal heterogeneity changes that occurred during colony spreading. Therefore, those changes

introduce a new variable that influences the dynamics of the biological interface.

On the other hand, previous work on the spreading dynamics of bacterial colonies, such as *Escherichia coli* and *Bacillus subtilis* in agar-containing media [3], revealed a nontrivial value for the roughness exponent, $\alpha = 0.78 \pm 0.07$, a figure exceeding the value predicted by the standard KPZ model. At this stage, the study of the growth dynamics of silver 2D electrodeposits in non-Newtonian media with different concentrations of agarose [15,16] revealed a set of scaling exponents that depended on the structure of the media. More recently, it was shown that the universal behavior of bacterial colonies could be more complex than previously thought due to the appearance of quenched disorder in growth patterns depending on the nutrient concentration regime [4]. At variance with bacteria, in the case of cell line colonies data on the influence of the medium properties on the front propagation dynamics remain an important matter for further research, particularly for modeling complex biological processes such as tumor growth [17].

In this work, the 2D front spreading dynamics of Vero cell colonies in a gelled culture medium was investigated utilizing the dynamic scaling theory. A standard culture medium was gelled by the addition of methylcellulose (MC). MC is a hydrophilic polymer yielding a clear, nonadhesive, viscous (non-Newtonian) solution that thickens the medium without being toxic to the cells. It has been employed, for instance, in cell cultures to study viral replication processes [18,19]. Data on Vero cell colonies embedded in MC-containing medium, with a constant nutrient concentration, are compared to those reported for MC-free medium [8,9]. This comparison discloses that in the MC-containing medium the occurrence of pinning effects interferes with the 2D colony front dynamics. The resulting set of exponents, within a certain range of colony size and age, becomes consistent with the spreading dynamics expected from the quenched Kardar-Parisi-Zhang (QKPZ) equation [1,2,14].

*mahuergo@inifta.unlp.edu.ar

†nicolasemuzzio@gmail.com

‡miguelp@inifta.unlp.edu.ar

§vukogon@gmail.com

‖aebolzan@inifta.unlp.edu.ar

¶ajarvia@inifta.unlp.edu.ar

II. EXPERIMENT

A. Preparation of cell colonies

Vero cells (passages 165–180) were cultured initially in Roswell Park Memorial Institute (RPMI 1640) standard medium containing 10% fetal bovine serum, under a 5% carbon dioxide atmosphere at 37°C and 97% humidity. It should be noted that the colonies were initially grown in MC-free medium because the presence of MC in the medium at the very beginning prevented the cells from adhering to the petri dish and reproducing to attain the critical population that is always needed for growth of the colony. In all cases, cell viability was routinely checked employing the exclusion Trypan Blue test, and cell proliferation examined with the nuclear cell proliferation antigen Ki-67 from Dako.

MC-containing culture medium was prepared by mixing RPMI medium containing 20% fetal bovine serum, aqueous 5% MC (Sigma Aldrich; approximate molecular weight, 14 000; catalog no. M7027) solution (250 cps dynamic viscosity), and the appropriate amount of water to obtain a 2.5% MC gel culture medium (≈25 cps dynamic viscosity). MC with an intermediate degree of substitution of OH by methoxy groups in cellulose favors soluble species presumably forming a "cagelike" structure surrounding hydrophobic methoxy groups [20–22].

Quasilinear front colonies were made following a procedure that has been described earlier [9]. Briefly, two face-to-face quasilinear colony fronts of size (L) were formed at the bottom of a petri dish, leaving a free central region for the growth of the colony in MC-free medium. After 24 h, the culture medium was replaced with the MC-containing one and the continuous displacements in opposite directions of both colony fronts starting at $t = t_0$ were followed up.

B. Colony growth pattern imaging

Colony images were obtained with a Canon digital camera coupled to a Nikon TS100 phase-contrast inverted microscope with a CFI flat-field ADL 10× objective at a resolution of 0.88 μm/pixel. Colony fronts were manually traced using a Wacom graphic tablet. Traces of colony growth patterns were drawn from computer screen images by selecting the most convenient zooming. As reported elsewhere [8] the trace error was of the order of a pixel.

The follow-up of colony growth patterns was extended for about 12 days, the time at which collapse of the colony front with an isolated free cell cluster in the medium became possible. Image analysis was made from sequential images taken *in situ* or from colonies fixed and stained with May-Grunwald-Giemsa after growth at different selected times.

C. Dynamic scaling analysis of 2D colony fronts

The dynamic scaling analysis of sequential 2D colony front data was made by employing an in-laboratory-developed program that provided $h_i(t)$, the instantaneous distance from the *i*th point at the colony front ($i = 1, 2, \ldots, N$) to the baseline of the colony, the average distance, $\langle h \rangle = \sum h_i/N$, and the instantaneous global and local roughness. Both the global [$w(L,t)$] and the local [$w(l,t)$] colony front roughness were determined from overhang-corrected data. The influence of

this correction, which was required for the short-size front roughness scaling, became practically null as the colony front length exceeded 3–4 average cell diameters (ca. 100 μm). The overhang-corrected profiles were obtained by taking the maximal value of $h_i(t)$ at each point i, as reported in Refs. [8] and [9].

The instantaneous front roughness, $w(L,t)$, was determined from the standard deviation of the front height fluctuations,

$$w(L,t) = \left[\frac{1}{N} \Sigma [h_i(t) - \langle h(t) \rangle]^2 \right]^{1/2}, \qquad (1)$$

where L is the length of the growing front. The colony front roughness depended on both the colony growth time and the local front size (l, with $l \leqslant L$) [1,8]. The local instantaneous roughness, $w(l,t)$, was evaluated from the standard deviation of h_i for different front length portions l.

Starting from a flat surface, the value of $w(L,t)$ for $t \ll t_s$, t_s being the roughness saturation time, is expected to increase as

$$w(L,t) \propto t^\beta \quad (t \ll t_s), \qquad (2)$$

with β being the growth exponent. Then, for a fixed value of L the front roughness should reach a saturation value at t_s. Otherwise, if L is changed, $w_s(L,t)$, the saturation roughness, should depend on L according to

$$w_s(L) \propto L^\alpha \quad (t \gg t_s), \qquad (3)$$

with α being the roughness exponent. The value of t_s depends on the system size as [1]

$$t_s \propto L^z, \qquad (4)$$

where z is the dynamic exponent. In Eqs. (2) and (3) β governs the interface roughening short-time behavior, whereas α characterizes the stationary regime.

From Eqs. (2) and (3), the size and time dependence of $w(L,t)$ fulfills the Family-Vicsek dynamic scaling relationship [23]

$$w(L,t) \propto L^\alpha f\left(\frac{t}{L^z} \right), \qquad (5)$$

the scaling function $f(x = tL^{-z})$ being

$$f(x) = \begin{cases} \text{const} & \text{for} \quad x \gg 1, \\ x^\beta & \text{for} \quad x \ll 1. \end{cases} \qquad (6)$$

The exponents β, α, and z are linked through $z = \alpha/\beta$. Equation (5) should bring about the collapse of roughness data, resulting in a single universal curve [1].

The more general dynamic scaling theory based on the analysis of the structure factor of the interface [$S(k,t)$] introduces α_s, a spectral roughness independent exponent that takes into account other dynamic scaling analysis features, through the expression [24]

$$S(k,t) = \langle \hat{h}(k,t)\hat{h}(-k,t) \rangle, \qquad (7)$$

where

$$\hat{h}(k,t) = \frac{1}{\sqrt{L}} \sum_x [h(x,t) - \langle h \rangle] e^{ikx} \qquad (8)$$

is the kth Fourier mode of front height fluctuations around its average value at t. Then the general scaling relationship in

terms of $S(k,t)$ is [24]

$$S(k,t) = k^{-(2\alpha_s+1)} f(kt^{1/z}), \tag{9}$$

with $f(x = kt^{1/z})$ being a scaling function that depends on x as

$$f(x) = \begin{cases} \text{const} & \text{for} \quad x \gg 1, \\ x^{(2\alpha_s+1)} & \text{for} \quad x \ll 1. \end{cases} \tag{10}$$

From the slope of the $S(k,t)$ versus k plots the value of α_s is obtained, which allows anomalous roughening processes to be distinguished when $\alpha_s \neq \alpha$ [24].

III. RESULTS AND DISCUSSION

The colony pattern morphology of quasilinear fronts in the gel medium at early stages of growth showed domains of small cells with sharp tips and, at about 4000 min, the occurrence of slow-moving enlarged cells (Fig. 1). The average cell diameter in the front region increases from about 45 μm at $t = 2400$ min to about 250 μm at $t = 19\,620$ min, i.e., a value fourfold greater than that found for the largest cells produced in MC-free medium [8].

Application of the Ki-67 test to cell colonies growing in the gel culture medium showed that only clusters of small cells were under duplication; i.e., the colony population exhibits a sluggish duplication rate compared to those colonies in MC-free medium [8]. On the other hand, the Trypan Blue test demonstrated that the large cells, although not duplicating, were viable, i.e., they remained active along the duration of each experiment. Presumably, the presence of MC makes it more difficult to access growth factors from the medium to the cells, their transport being slowed down by both the high dynamic viscosity and the proper network structure of the gelled medium [25]. Nevertheless, the colony front displaces at a constant velocity, $\langle v_F \rangle = 0.126 \pm 0.003$ μm min^{-1} (Fig. 2), a figure about one-half the value earlier reported for MC-free medium [8].

Sequential patterns of colonies growing in the gelled medium (Fig. 3) show that the enlarged cells behave like slow-moving obstacles quenching the displacement of smaller neighbor cells, particularly those moving towards the colony front. Correspondingly, these obstacles should disturb the
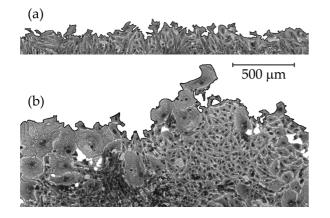

FIG. 1. Images of a quasilinear colony front region for different growth times after fixing and staining: (a) 2400 min; (b) 19 600 min. Black dots correspond to cell nuclei.
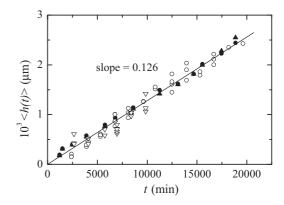

FIG. 2. Average colony front height versus growth time. Symbols correspond to different experiments.

velocity components of each cell to comply with their adequate trajectory towards the colony front.

Dynamic scaling data plotted as $w(L,t)$ versus t log-log plots (Fig. 4) fulfill a fairly good straight line with the slope $\langle \beta \rangle = 0.75 \pm 0.03$ within the 4000- to 15 000-min range. Conversely, the $w(l,t)$ versus t log-log plots (Fig. 5) display a set of lines that shift upward as either l (at constant t) or t (at constant l) is increased.

For these colonies the value of $w(l,t)$ remains almost constant for about 3000 min, i.e., within an interval in which the morphology of the colony remains almost unchanged, and
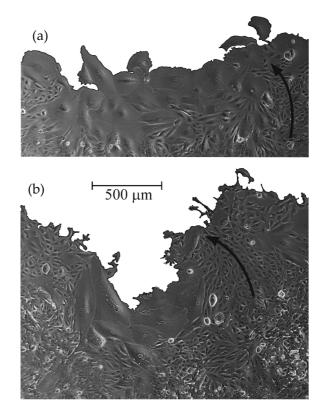

FIG. 3. Sequential images of a quasilinear colony front region taken at (a) $t = 14\,595$ min and (b) $t = 20\,370$ min. The coarse trajectory displacement of regular cells around a cluster of enlarged ones during growth is indicated by the arrows.
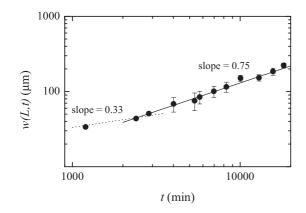
FIG. 4. Colony front roughness versus growth time log-log plot. Data from different colonies have been binned.

the number of cell duplications becomes very scarce. Later, for $l < 900$ μm, within the range $4000 \leqslant t \leqslant 10\,000$ min, the w versus t plot fulfills a straight-line relationship with $\langle\beta\rangle = 0.75 \pm 0.06$, a figure compatible with that given above. Furthermore, in the $100 \leqslant l \leqslant 1200$ μm range, those plots approach a roughness saturation value, w_s, associated with the saturation time, t_s, that increases with l. The t_s versus l_s log-log plot (Fig. 5, inset) yields a straight-line relationship with a slope $z = 0.80 \pm 0.025$, in good agreement with the z exponent obtained from the quotient α/β [1].

Data displayed in Fig. 5 involve two limiting linear behaviors: one at the lowest l values, in the $3000 \leqslant t \leqslant 12\,000$ min range, with a lower slope, probably close to 0.33, i.e., the value of β expected from the standard KPZ model, and another one at the highest values of l and t, with slope $\langle\beta\rangle = 0.75 \pm 0.05$. This figure indicates an increase in the

FIG. 6. Colony (a) front roughness versus front width l and (b) $S(k,t)$ versus k log-log plots for different colony growth times. The line with slope -2.26 (i.e., $\langle\alpha_S\rangle = 0.63$) is a guide for the eye. Data have been binned.

roughness change rate, in agreement with the observations of the colony front pattern images (Figs. 1 and 3). These results are consistent with the the accumulation of enlarged cells at the colony border region, forming a sort of permeable barrier for the displacement of small cells towards the colony front.

The $w(l,t)$ versus l log-log plots display a straight-line region approaching the slope $\langle\alpha\rangle = 0.63 \pm 0.04$ that extends from $l \approx 100$ μm over ranges of l that increase with t [Fig. 6(a)]. For $l > 10\,000$ μm, the trend of $w(l,t)$ to attain a saturation value is noted.

On the other hand, the $S(k,t)$ versus k log-log plot approaches the common average slope -2.26, which implies a spectral roughness exponent $\langle\alpha_s\rangle = 0.63 \pm 0.02$ [Fig. 6(b)]. The fairly close coincidence of the values of $\langle\alpha\rangle$ and $\langle\alpha_S\rangle$ indicates the absence of anomalous roughening [24]. Correspondingly, the value of $\langle z\rangle = \langle\alpha\rangle/\langle\beta\rangle = 0.83 \pm 0.05$ furnishes a reasonably good collapse of the roughness data, as predicted by the Family-Vicsek relationships [1,24] (Fig. 7).

In principle, the set of dynamic scaling exponents suggests that the 2D colony spreading in the gel medium under constant $\langle v_F\rangle$ is consistent with a random contribution of pinning forces in the process [1]. As previously reported [8,9], the 2D dynamics of Vero cell colony fronts in MC-free medium
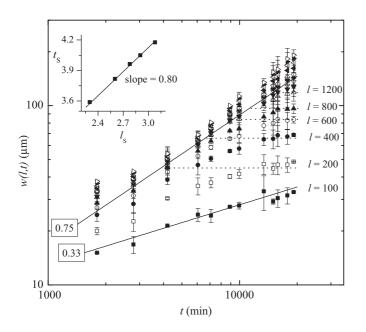

FIG. 5. Colony front roughness versus colony growth time log-log plots for different front widths l, as indicated. Straight lines with slopes 0.33 and 0.75 are displayed to guide the eye. Inset: Corresponding t_s versus l_s log-log plot.
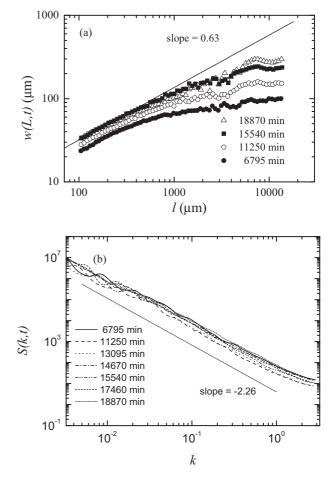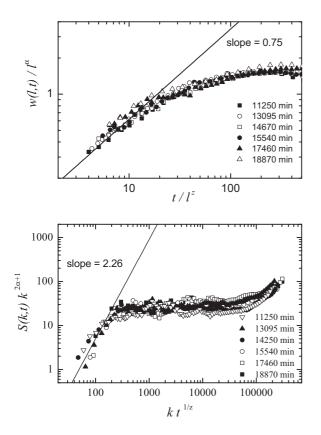
FIG. 7. Log-log plots of Family-Vicsek scaling relationships at various growth times as indicated. Data have been binned.

formally approach the prediction of the standard KPZ equation within certain ranges of l and t. Conversely, data resulting from the gel medium show an exponent α exceeding the predictions of the KPZ class. Such large α exponents are usually found in systems with different stochastic terms, such as non-Gaussian thermal noises or quenched noises. In this case the KPZ standard equation has been modified by introducing a quenched disorder $\eta(x,h)$ instead of the noise term $\eta(x,t)$ [26],

$$\frac{\partial h(x,t)}{\partial t} = \nu \nabla^2 h + \frac{\lambda}{2}(\nabla h)^2 + F + \eta(x,h), \qquad (11)$$

which has been denoted the QKPZ equation. As in the standard KPZ equation, the first term on the right-hand side in Eq. (11) describes the relaxation of the interface (smoothing) caused by ν, a surface tension contribution that tends to reduce irregularities at the rough profile, changing the average protrusion height. The smoothing process may also involve diffusion of cells. F is a driving force mainly generated by the cooperation of cell proliferation and cell size increase in the colony. The nonlinear term $\lambda(\nabla h)^2$ accounts for the lateral growth of protrusions and breaks the up-down symmetry such that the interface is no longer invariant under the transformation $h \to -h$. In this case, the addition of material from either cell duplication or cell size increase and the cell displacements in the colony bulk at lateral parts of protrusions, where the local slope is larger, increase the average height of the colony front. The term $\eta(x,h)$, which is responsible for the global pinning, has short-range correlations, i.e., $\langle \eta(x,h)\eta(x',h') \rangle =$

$\delta(x - x')\triangle(h - h')$. Accordingly, the large value of α reported in this work would be related to the quenched disorder introduced by strong lateral interactions resulting from both the occurrence of large cells, particularly at the colony front, and the characteristics of the gelled structured medium.

For QKPZ dynamics, as there is no pinning-depinning transition in the $\langle h \rangle$ versus t plots (Fig. 2), the interface moves with a finite velocity under F from the very beginning. Quenched models have been extensively studied for 1D condensed phase growth and used, for instance, to describe the interfacial behavior of directed percolation depinning models [27–30]. Numerical calculations and the simulation of an automaton model also showed that $\alpha = 0.63$ [31]. Self-organized growth models have also been proposed to study the dynamics of random interfaces in random media [30]. One of these models, denoted model B, also predicted $\alpha = 0.63 \pm 0.02$ and $\beta = 0.9 \pm 0.1$.

The above results indicate that seemingly the 2D spreading dynamics of Vero cell colonies changes from a KPZ behavior in MC-free standard medium [8,9] to a QKPZ in MC-containing gel medium. However, despite the rather good agreement between the experimental data and the QKPZ model, within the ranges of l and t studied in this work, the occurrence of enlarged cells during the colony spreading appears to be a relevant variable that deserves further attention in modeling the interfacial dynamics of biological systems.

IV. CONCLUSIONS

In MC-containing gelled culture medium, 2D Vero cell colony front spreading occurs at a velocity lower than that in standard MC-free medium. This effect is due to the influence of MC on the medium, which drastically changes its structural characteristics and contributes to the decrease in the cell duplication rate, presumably favoring the occurrence of large cells that hinder cell motility in the colony. Large cells at the colony border behave as pinning sites for the displacement of small cells towards the front. From the dynamic scaling analysis, the set of exponents $\alpha = 0.63 \pm 0.04$, $\beta = 0.75 \pm 0.05$, and $z = 0.84 \pm 0.05$ was obtained. This set is consistent with the presence of a quenched disorder at the colony front influencing the dynamics of the biological interface. This set of exponents is predicted by the quenched KPZ universality class. By comparing the present data with data reported earlier for a standard MC-free culture medium, it can be concluded that whereas the spreading dynamics of Vero cell colonies in the former case fit the standard KPZ model, in the gelled medium it fits the QKPZ universality class. This conclusion should be cautiously considered because of the restricted range of the experimental data in which comparison with models becomes possible and the validity of extending to biological systems those frameworks underlying condensed phase growth models.

[1] A. L. Barabasi and H. E. Stanley, *Fractal Concepts in Surface Growth* (Cambridge University Press, Cambridge, 1995).

[2] P. Meakin, *Fractals, Scaling and Growth Far from Equilibrium* (Cambridge University Press, London, 1998).

[3] T. Vicsek, M. Cserzo, and V. K. Horvath, Physica A **167**, 315 (1990).

[4] J. A. Bonachela, C. D. Nadell, J. B. Xavier, and S. A. Levin, J. Stat. Phys. **144**, 303 (2011).

[5] A. Brú, J. M. Pastor, I. Fernaud, I. Brú, S. Melle, and C. Berenguer, Phys. Rev. Lett. **81**, 4008 (1998).

[6] A. Brú, S. Albertos, J. L. Subiza, J. L. García-Asenjo, and I. Brú, Biophys. J. **85**, 2948 (2003).

[7] M. Block, E. Schöll, and D. Drasdo, Phys. Rev. Lett. **99**, 248101 (2007).

[8] M. A. C. Huergo, M. A. Pasquale, A. E. Bolzán, A. J. Arvia, and P. H. González, Phys. Rev. E **82**, 031903 (2010).

[9] M. A. C. Huergo, M. A. Pasquale, P. H. González, A. E. Bolzán, and A. J. Arvia, Phys. Rev. E **84**, 021917 (2011).

[10] M. A. C. Huergo, M. A. Pasquale, P. H. González, A. E. Bolzán, and A. J. Arvia, Phys. Rev. E **85**, 011918 (2012).

[11] J. Galeano, J. Buceta, K. Juárez, B. Pumariño, J. de la Torre, and J. M. Iriondo, Europhys. Lett. **63**, 83 (2003).

[12] K. A. Takeuchi and M. Sano, Phys. Rev. Lett. **104**, 230601 (2010).

[13] K. A. Takeuchi and M. Sano, J. Stat. Phys. **147**, 853 (2012).

[14] T. Halpin-Healy and Y.-C. Zhang, Phys. Rep. **254**, 215 (1995).

[15] M. A. Pasquale, J. L. Vicente, S. L. Marchiano, and A. J. Arvia, J. Phys. Chem. B **108**, 13315 (2004).

[16] M. A. Pasquale, S. L. Marchiano, and A. J. Arvia, in *Thinking in Patterns, Fractals, and Related Phenomena in Nature*, edited by M. M. Novak (World Scientific, Singapore, 2004), p. 267.

[17] L. Preziosi, *Cancer Modeling and Simulation* (Chapman and Hall CRC, New York, 2003).

[18] R. Risser and R. Pollack, Virology **59**, 477 (1974).

[19] T. Ito, Y. Ishikawa, S. Okano, T. Hattori, R. Fujii, T. Shinozawa, and A. Shibuya, Cancer Res. **47**, 4146 (1987).

[20] A. Haque and E. R. Morris, Carbohydr. Polym. **22**, 161 (1993).

[21] N. Sarkar, Carbohydr. Polym. **26**, 195 (1995).

[22] K. Kobayashi and C.-I. Huang, Macromolecules **32**, 7070 (1999).

[23] F. Family and T. Vicsek, J. Phys. A **18**, L75 (1985).

[24] J. J. Ramasco, J. M. López, and M. A. Rodríguez, Phys. Rev. Lett. **84**, 2199 (2000).

[25] L. Li, P. M. Thangamathesvaran, C. Y. Yue, K. C. Tama, X. Hu, and Y. C. Lam, Langmuir **17**, 8062 (2001).

[26] G. Parisi, Europhys. Lett. **17**, 673 (1992).

[27] L.-H. Tang and H. Leschhorn, Phys. Rev. Lett. **70**, 3832 (1993).

[28] S. V. Buldyrev, A. L. Barabasi, F. Caserta, S. Havlin, H. E. Stanley, and T. Vicsek, Phys. Rev. A **45**, R8313 (1992).

[29] L.-H. Tang and H. Leschhorn, Phys. Rev. A **45**, R8309 (1992).

[30] K. Sneppen, Phys. Rev. Lett. **69**, 3539 (1992).

[31] H. Leschhorn, Phys. Rev. E **54**, 1313 (1996).